Proceedings of the 16th International Heat Transfer Conference, IHTC-16
August 10-15, 2018, Beijing, China

IHTC16-22069

MAGNETIC RESONANCE THERMOMETRY DURING THE LOCALIZED HEATING OF BIOLOGICAL TISSUES

Cesar C. Pacheco[1*], Helcio R. B. Orlande[1], Marcelo J. Colaço[1], George S. Dulikravich[2], Leonardo A. B. Váron[3]

[1] Department of Mechanical Engineering, Federal University of Rio de Janeiro – POLI/COPPE, Centro de Tecnologia, Caixa Postal: 68503, Cidade Universitária, Rio de Janeiro, 21941-972, Brazil
[2] Department of Mechanical and Materials Engineering, MAIDROC Laboratory Florida International University, 10555 West Flagler St., EC 3462, Miami, Florida 33174, USA
[3] Department of Bioengineering, University of Santiago de Cali, Colombia

ABSTRACT

In this paper, a state estimation problem is solved with the Steady-State Kalman filter for the nonintrusive measurements of the temperature inside the human body, with the magnetic resonance technique. The paper is focused on temperature measurements during the hyperthermia treatment of cancer imposed by radiofrequency waves. The coupled bioheat transfer and electromagnetic problems are numerically solved in a realistic two-dimensional geometry obtained from the Visual Human Dataset. The tumor is considered loaded with nanoparticles in order to improve the localized absorption of the radiofrequency waves and to avoid the undesired heating of healthy tissues. Numerical results demonstrate that the present Steady-State Kalman filter solution is more accurate than the direct data inversion, which is commonly used for recovering the local transient temperature variation from the magnetic resonance measurements.

KEY WORDS: Inverse Problems, Heat transfer enhancement, Nanoparticles, Hyperthermia

1. INTRODUCTION

In the hyperthermia treatment of cancer, the temperature of the tumour is increased in order to induce cell necrosis (commonly referred to as thermoablation) or to improve the sensitivity of the cells to cytotoxic agents, like chemotherapeutic drugs or radiation [1,2]. As for other kinds of treatments, damages to the healthy cells is of major concern. However, with the recent technological advances, nanoparticles have been used to improve the localized heating of the tumour, due to their enhanced absorption of electromagnetic waves caused by surface plasmon resonance [1-6].

Prior planning and control strategies are needed for the hyperthermia treatment of cancer. For both cases, computational simulations under the effects of uncertainties are required, which must take into account the physical phenomena involved in the heating process, like the interaction of electromagnetic waves with tissues, blood perfusion and metabolic heat generation, among others. In special, control strategies require real-time accurate knowledge of the temperature in the heated region, in order to avoid thermal damage to healthy cells. Several techniques have been developed for the measurement of the temperature inside the human body, including the Magnetic Resonance Thermometry (MRT) [1,2,7,8]. Although this technique has been successfully used in practice, related uncertainties can be reduced by coupling this kind of measurement with the mathematical model of the physical problem and by solving a state estimation problem [9-12], as demonstrated for an arbitrary heating in [13]. In this paper, we extend our previous work [13] and couple the bioheat transfer problem to the heating problem imposed by the external application of waves in the

*Corresponding Author: cesar.pacheco@poli.ufrj.br

radiofrequency range. The state estimation problem is solved with an asymptotic version of the Kalman filter, referred to as the Steady-State Kalman filter [12], which provides a significant reduction on the required computational effort.

2. MAGNETIC RESONANCE THERMOMETRY

Different techniques can be found in the literature for nonintrusive temperature measurements via magnetic resonance. However, the PRF-Shift technique developed by Ishihara *et al.* [14] outperforms the other available techniques [2,7,15]. The basic principle of the PRF-Shift technique is that specific atomic nuclei possess a natural magnetic moment due to spin [16]. When an external magnetic field $\mathbf{B}_0$ is applied to such nuclei, they start a precession movement around the axis of $\mathbf{B}_0$. This precession movement has a well-defined frequency, which is called *Larmor frequency*, given by [16]:

$$\omega(\mathbf{r}) = \gamma B_{nuc}(\mathbf{r}) \tag{1}$$

where γ is the gyromagnetic ratio. The magnitude of the magnetic field in the vicinity of the atomic nuclei, $B_{nuc}(\mathbf{r})$, is not equal to the magnitude of the external magnetic field, $B_0(\mathbf{r})$, due to the nuclear shielding performed by the electron cloud [16]. The magnetic field produced by this shielding is proportional to $B_0(\mathbf{r})$, so that the local magnetic field at the nuclei can be written as [16]:

$$B_{nuc}(\mathbf{r}) = \left[1 - s(\mathbf{r})\right] B_0(\mathbf{r}) \tag{2}$$

where $s(\mathbf{r})$ is the *chemical shift*. It was shown that the chemical shift is temperature dependent, that is, $s(\mathbf{r}) \equiv s(\mathbf{r},T)$ [14]. Moreover,

$$\frac{\partial s}{\partial T} = \alpha \tag{3}$$

is constant for a wide range of temperatures (in special those for hyperthermia treatment applications) and practically independent of the tissue, except for fat [2,7,13,16,17]. Therefore, the local phase shift from a reference angular value, $\Delta\Phi(\mathbf{r},T)$, can be obtained for the precession movement as:

$$\Delta\Phi(\mathbf{r},T) = \gamma\left[1 - s(\mathbf{r},T)\right] B_0(\mathbf{r}) t_{TE} \tag{4}$$

where t_{TE} is the time interval used to measure the phase shift through Gradient Echo sequences [2,14], also known as the echo-time [19,20]. The phase shift is then measured for two different temperatures, including the baseline temperature before the heating process, $T_0(\mathbf{r})$, and the temperature $T(\mathbf{r},t)$ during the heating. By using equations (3) and (4) we can write:

$$T(\mathbf{r},t) - T_0(\mathbf{r}) = -\frac{\delta(\mathbf{r},t)}{\alpha\gamma t_{TE} B_0} \tag{5}$$

where

$$\delta(\mathbf{r},t) = \Delta\Phi(\mathbf{r},T) - \Delta\Phi(\mathbf{r},T_0) \tag{6}$$

Equation (5) provides a relation between the temperature variation $\Delta T(\mathbf{r},t) = T(\mathbf{r},t) - T_0(\mathbf{r})$ and the resulting phase variation. Therefore, from the magnetic resonance measurements of $\delta(\mathbf{r},t)$, the temperature variation can be directly inferred from equation (5). This *direct inversion* is commonly used in practice for measuring temperature variations with the PRF-Shift method [20].

3. BIOHEAT TRANSFER MODEL

The bioheat transfer problem is described in this work by the Pennes model [21], with convective boundary conditions at the body surfaces and an initial condition given by the baseline temperature $T_0(\mathbf{r})$. The mathematical formulation for the temperature variation $\Delta T(\mathbf{r},t)$ is thus given by:

$$\rho(\mathbf{r})c_p(\mathbf{r})\frac{\partial \Delta T}{\partial t} = \nabla\cdot\left[k(\mathbf{r})\nabla(\Delta T)\right] - \omega\rho_b c_b \Delta T(\mathbf{r},t) + g_h(\mathbf{r}), \quad \mathbf{r}\in\Omega,\ t>0 \tag{7}$$

$$k(\mathbf{r})\frac{\partial \Delta T}{\partial \mathbf{n}} + h\Delta T = 0, \quad \mathbf{r}\in\partial\Omega,\ t>0 \tag{8}$$

$$\Delta T(\mathbf{r},t) = 0, \quad \mathbf{r}\in\Omega,\ t=0 \tag{9}$$

The baseline temperature is the solution of the steady-state bioheat transfer problem before heating takes place, that is,

$$\nabla\cdot\left[k(\mathbf{r})\nabla T_0\right] + \omega\rho_b c_b\left[T_a - T_0(\mathbf{r})\right] + g_m(\mathbf{r}) = 0, \quad \mathbf{r}\in\Omega \tag{10}$$

$$k(\mathbf{r})\frac{\partial T_0}{\partial \mathbf{n}} + hT_0 = hT_\infty, \quad \mathbf{r}\in\partial\Omega \tag{11}$$

In equation (7), $g_h(\mathbf{r},t)$ is the heat source term that results from the external heating. In this work, radiofrequency waves are used to increase the temperature of the body tissues in a hyperthermia treatment of cancer, such as in [22,23]. The tumor region is supposed to be loaded with iron oxide (Fe_3O_4) nanoparticles, in order to locally increase absorption of the radiofrequency waves and avoid thermal damage to the healthy cells. The heat generation term can be written as [22,23]:

$$g_h(\mathbf{r}) = \left\{\left[1-\theta(\mathbf{r})\right]\frac{\sigma(\mathbf{r})}{2} + \theta(\mathbf{r})\left(\frac{9}{16}\frac{\chi''}{\mu_0\pi f R^2}\right)\right\}\left|\mathbf{E}(\mathbf{r})\right|^2 \tag{12}$$

where $\theta(\mathbf{r})$ is the local volumetric concentration of nanoparticles. The electric field $\mathbf{E}(\mathbf{r})$ is given by

$$\mathbf{E}(\mathbf{r}) = -\nabla u(\mathbf{r}) \tag{13}$$

The problem for the calculation of the electric potential $u(\mathbf{r})$ in the body is given by [22,23]:

$$\nabla\cdot\left[\varepsilon(\mathbf{r})\nabla u(\mathbf{r})\right] = 0, \quad \mathbf{r}\in\Omega \tag{14}$$

$$u = u^+, \quad \mathbf{r}\in\partial\Omega_1 \tag{15}$$

$$u = u^-, \quad \mathbf{r}\in\partial\Omega_2 \tag{16}$$

$$\frac{\partial u}{\partial \mathbf{n}} = 0, \quad \mathbf{r}\in\partial\Omega_3\cup\partial\Omega_4 \tag{17}$$

where the boundary surfaces $\partial\Omega_1$ and $\partial\Omega_2$ correspond to the electrodes maintained at the voltages u^+ and u^-, respectively. Electrical current is assumed null at the remaining boundary surfaces.

4. STATE ESTIMATION PROBLEM

A state estimation problem is solved in this work to recover the transient temperature variation $\Delta T(\mathbf{r},t)$ and avoid that uncertainties in the magnetic resonance measurements be directly propagated to the temperature variation, such as in the direct inversion given by equation (5). State estimation problems are solved within the Bayesian framework, where the unknown states of a system are sequentially estimated based on the mathematical formulations of the physical problem and of the measurement system, as well as on the measurements themselves [9-12].

In this work, the state and observation vectors are given, respectively, by the local temperature increase and by the phase-shift, in each finite control volume used for the discretization of the body, that is,

$$\mathbf{x}_n = \Delta\mathbf{T}_n \tag{18}$$

$$\mathbf{y}_n = \boldsymbol{\delta}_n \tag{19}$$

where the subscript n represents the time $t_n = n\Delta t$. The evolution and observation models are linear and their related uncertainties are modeled here as Gaussian, additive, with zero mean and constant covariance matrix, such as in [13]. Therefore, we can write

$$\mathbf{x}_n = \mathbf{F}_n\mathbf{x}_{n-1} + \mathbf{u}_n + \mathbf{w}_n \tag{20}$$

$$\mathbf{y}_n = \mathbf{H}_n\mathbf{x}_n + \mathbf{v}_n \tag{21}$$

with $\mathbf{w}_n \sim N(\mathbf{0}, \mathbf{Q}_n)$ and $\mathbf{v}_n \sim N(\mathbf{0}, \mathbf{R}_n)$. In this work, the external heating term is not modelled as part of the state vector, but rather as a control vector, $\mathbf{u}$. The matrix $\mathbf{F}$ results from the discretization of the bioheat transfer problem with the finite volume method [13]. By assuming that the measurements are available at every finite volume used for the discretization, we can write (see equation 5):

$$\mathbf{H}_n = -\alpha\gamma t_{\mathrm{TE}} B_0 \mathbf{I} \tag{22}$$

The optimal solution of linear and Gaussian evolution and observation models, such as those given by equations (20) to (22), can be obtained with the recursive equations of the Kalman filter [9-12, 23, 24]. Despite these sequential estimates being unbiased and with minimum variances, the implementation of the Kalman filter can result in computational times too large to allow its application for real-time processes, like the estimation of the temperature variation inside bodies that is aimed in this work. The number of operations performed with the Kalman filter are of the order of N^3, where N is the number of state variables. On the other hand, an asymptotic version of the Kalman filter is available for time-invariant systems, where the evolution and observation matrices, $\mathbf{F}$ and $\mathbf{H}$, respectively, as well as the covariance matrices $\mathbf{Q}$ and $\mathbf{R}$, are not time dependent. This version is denoted as Steady-State Kalman filter, with associated number of operations of the order of N^2 [12]. Although not being the optimal solution, accurate estimates of the state variables could be obtained with the Steady-State Kalman filter for a problem similar to the present one [13]. The equations for the Steady-State Kalman filter are given by [12]:

$$\mathbf{P}_\infty = \mathbf{F}\mathbf{P}_\infty\mathbf{F}^T - \mathbf{F}\mathbf{P}_\infty\mathbf{H}^T\left(\mathbf{H}\mathbf{P}_\infty\mathbf{H}^T + \mathbf{R}\right)^{-1}\mathbf{H}\mathbf{P}_\infty\mathbf{F}^T + \mathbf{Q} \tag{23}$$

$$\mathbf{K}_\infty = \mathbf{P}_\infty\mathbf{H}^T\left(\mathbf{H}\mathbf{P}_\infty\mathbf{H}^T + \mathbf{R}\right)^{-1} \tag{24}$$

$$\hat{\mathbf{x}}_n^+ = \left(\mathbf{I} - \mathbf{K}_\infty\mathbf{H}\right)\mathbf{F}\hat{\mathbf{x}}_{n-1}^+ + \mathbf{K}_\infty\mathbf{y} \tag{25}$$

We note that only equation (25) needs to be applied recursively, while equations (23) and (24) are solved offline. Equation (25) is a Discrete Algebraic Riccati Equation [12], which can be readily solved with subroutines openly available [25].

5. RESULTS

The case analyzed in this work involved a two-dimensional domain, given by a transversal cut of a right human forearm, obtained from the Visual Human Dataset [26] (see figure 1a). From this geometry, the domain Ω and its boundaries $\partial\Omega$ were obtained and discretized with an unstructured mesh, as shown by figure 1b, where green, light blue and dark blue represent skin, muscle and bones, respectively. The red circular region in figure 1b corresponds to a tumor. For the hyperthermia treatment of the tumor, electrodes positioned as illustrated by figure 1c were used to generate radiofrequency waves that propagate inside the medium, with $u^+ = 4.5$ V and $u^- = 0$ V, at $\partial\Omega_1$ and $\partial\Omega_2$, respectively. Properties required for the solution of the problem given by equations (1) to (17) were obtained from references [13,22,23,27].

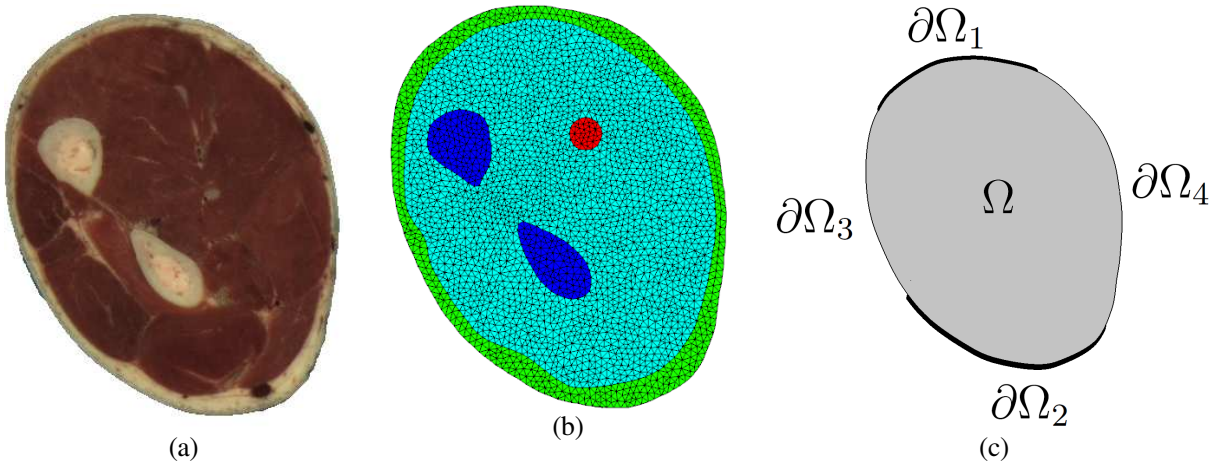

Fig. 1. Transversal cut of human right forearm: (a) PNG image, cropped from the Visual Human Dataset [26]; (b) Unstructured grid used for the finite volume solution; (c) Electrodes for the radiofrequency heating

Before examining the solution of the present state estimation problem, which aims at the estimation of the temperature field in the region presented by figure 1, it is interesting to notice the effect of applying nanoparticles to the tumor. Figures 2a and 2b present the heat source $g_h(\mathbf{r})$ resulting from the radiofrequency waves imposed to the region, for the cases without and with nanoparticles loaded to the tumor, respectively. While the heat source is more uniform and with smaller magnitude in the case without nanoparticles (see figure 2a), it is larger and concentrated in the tumor region for the case with nanoparticles (see figure 2b).

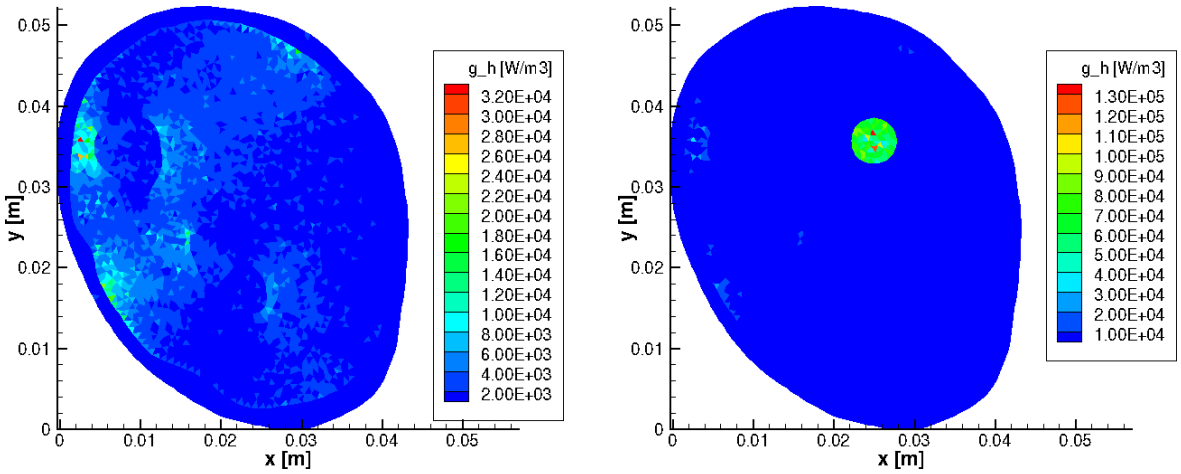

Fig. 2. Heat Source term $g_h(\mathbf{r})$ obtained from Eq. (12): (a) without nanoparticles; (b) with nanoparticles.

Simulated measurements were used for the solution of the present state estimation problem. They were generated from the direct problem solution for the case with nanoparticles loaded in the tumor and were considered available every 0.05 seconds, up to the final time of 60 seconds, in each control volume shown by figure 1b. The simulated measurements followed a Gaussian distribution with zero mean and constant standard deviation of 0.2°. The standard deviation of the uncertainties in the evolution model was also assumed as constant and equal to 0.05°C.

The exact temperature variation fields and the results obtained with the Steady-State Kalman filter for times t = 20 s, 40 s and 60 s are presented by figures 3, 4 and 5, respectively. Although some noise can be observed in the region with smaller temperature variations, the estimates are in excellent agreement with the exact temperature

variations in the tumor region. The tumor region is the one of most interest for the prediction of the temperature variations, since they are the focus of the hyperthermia treatment imposed by the radiofrequency waves, where the temperatures are then larger and the risk of thermal damage to the healthy cells is higher.

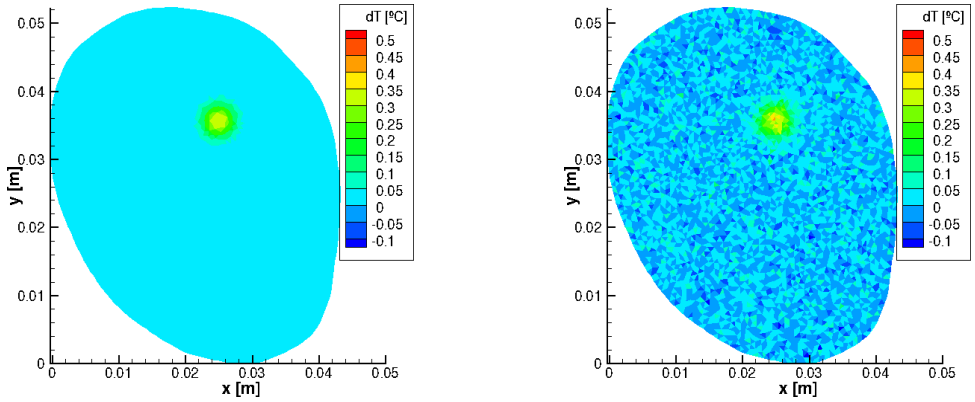

(a) (b)

Fig. 3 Temperature increase at $t = 20$ s: (a) exact; (b) estimated with SSKF.

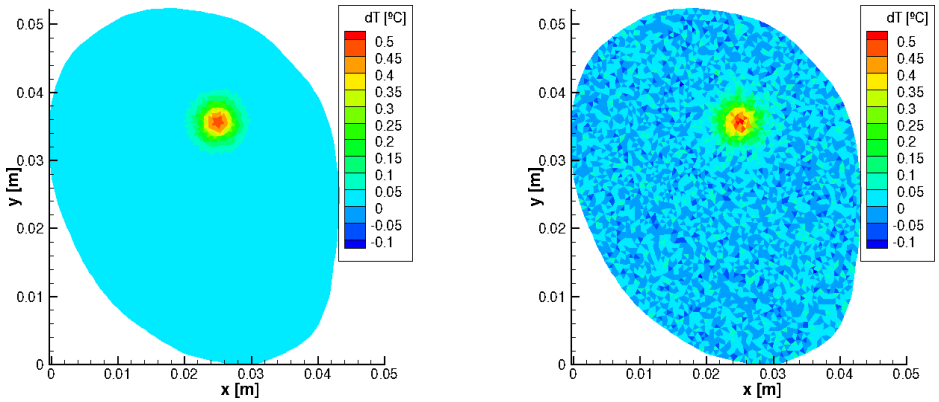

(a) (b)

Fig. 4. Temperature increase at $t = 40$ s: (a) exact; (b) estimated with SSKF.

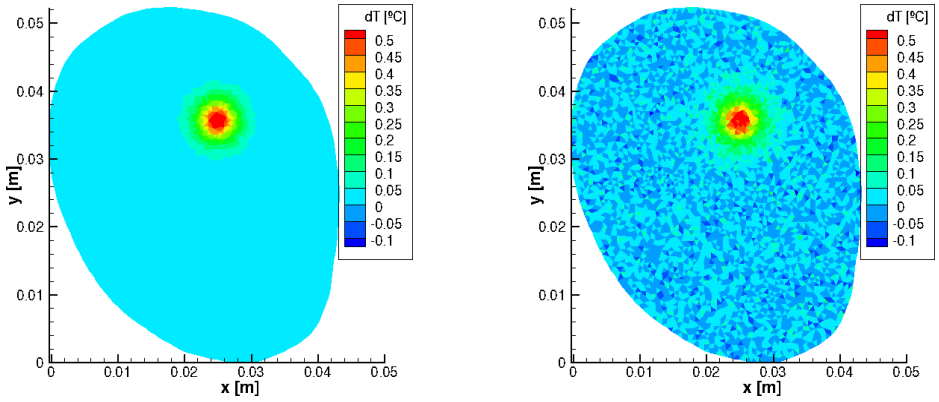

(a) (b)

Fig. 5. Temperature increase at $t = 60$ s: (a) exact; (b) estimated with SSKF.

The transient evolution of the temperature increase obtained by direct inversion of equation (5) and by the solution of the state estimation problem with the Steady-State Kalman filter, at the center of the tumor, are shown by figure 6a. This figure also shows the exact temperature variation and the 99% confidence intervals of the Steady-State Kalman filter solution. We notice in figure 6a that the temperature variation estimated with the

Steady-State Kalman filter is in much better agreement with the exact one, than that obtained by direct inversion of equation (5). Such fact becomes clearer from the analysis of figure 6b, which shows the errors between estimated and exact temperature variations, at the center of the tumor.

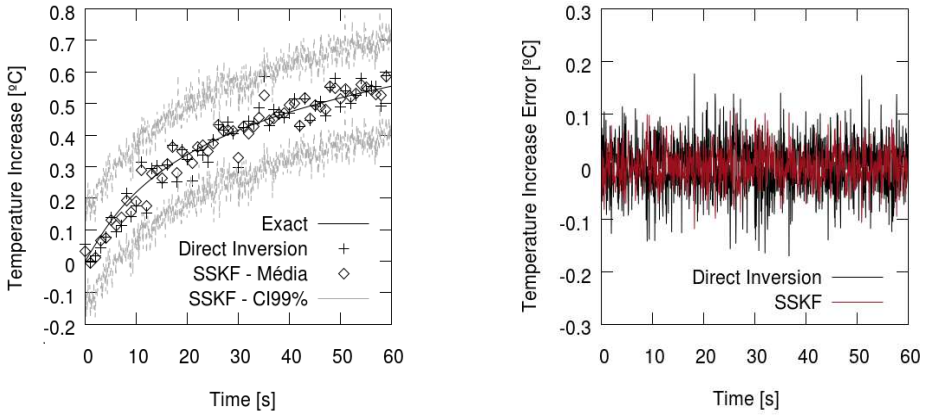

(a) (b)

Fig. 6. Transient variation of: (a) temperature increase estimates; (b) temperature increase error.

6. CONCLUSIONS

This paper presented the application of the Steady-State Kalman filter for the magnetic resonance thermometry of tissues in the human body, during the hyperthermia treatment of cancer. This work extends our previous results obtained with arbitrary heat sources, to a case where the heating was imposed by electromagnetic waves in the radiofrequency range. The tumor was supposed loaded with nanoparticles in order to concentrate the heating in the tumor region. The temperature variations estimated with the present approach were in much better agreement with the exact temperatures than the direct inversion commonly used in magnetic resonance thermometry. Estimation errors obtained with the Steady-State Kalman filter were smaller than 0.1 ^{o}C in the tumor region, which is the most critical during the hyperthermia treatment because healthy cells are more likely to undergo thermal damage due to the largest temperatures observed.

ACKNOWLEDGMENTS

This work was supported by Conselho Nacional de Desenvolvimento Científico e Tecnológico (CNPq), Coordenação de Aperfeiçoamento de Pessoal de Nível Superior (CAPES), Fundação Carlos Chagas Filho de Amparo a Pesquisa do Estado do Rio de Janeiro (FAPERJ) and Programa de Recursos Humanos da Agência Nacional de Óleo, Gás Natural e Biocombustíveis [ANP/PRH37].

NOMENCLATURE

c_p	specific heat	(J/kgºC)	T	temperature	(ºC)
f	RF heating frequency	(MHz)	T_a	arterial temperature	(ºC)
g_h	external heat source	(W/m³)	T_0	baseline temperature	(ºC)
g_m	metabolic heat source	(W/m³)	T_∞	environment temperature	(ºC)
h	heat transfer coefficient	(W/m²ºC)	t	time	(s)
k	thermal conductivity	(-)	**u**	control vector	(-)
R	radius of nanoparticles	(m)	u	electric potential	(V)
r	position vector	(-)	μ_0	magnetic permeability (vaccum)	(H/m)
σ	electrical conductivity	(S/m)	ρ	density	(kg/m³)
x	state vector	(-)	$\chi``$	magnetic susceptibility	(-)
y	observation vector	(-)	Ω	physical domain	(-)
			ω	blood perfusion coefficient	(s^{-1})

REFERENCES

[1] K. Hynynen et al., "A clinical, noninvasive, MR imaging-monitored ultrasound surgery method," RadioGraphics, vol. 16, no. 1, pp. 185–195, (1996).

[2] V. Rieke and K. Butts Pauly, "MR thermometry," J. Magn. Reson. Imaging, vol. 27, no. 2, pp. 376–390, (2008).

[3] Y. Bayazitoglu, "Nanoshell-assisted cancer thermal therapy: numerical simulations," in Proc 2nd ASME Micro/Nanoscale Heat & Mass Transfer: An International Conference, Shanghai, (2009).

[4] Y. Bayazitoglu, S. Kheradmand, and T. K. Tullius, "An overview of nanoparticle assisted laser therapy," Int. J. Heat Mass Transf., vol. 67, pp. 469–486, (2013).

[5] L. A. Dombrovsky, V. Timchenko, M. Jackson, and G. H. Yeoh, "A combined transient thermal model for laser hyperthermia of tumors with embedded gold nanoshells," Int. J. Heat Mass Transf., vol. 54, no. 25–26, pp. 5459–5469, (2011).

[6] L. A. Dombrovsky, V. Timchenko, C. Pathak, H. Piazena, W. Müller, and M. Jackson, "Radiative heating of superficial human tissues with the use of water-filtered infrared-A radiation: A computational modeling," Int. J. Heat Mass Transf., vol. 85, pp. 311–320, (2015).

[7] B. Denis de Senneville, B. Quesson, and C. T. W. Moonen, "Magnetic resonance temperature imaging," Int. J. Hyperth., vol. 21, no. 6, pp. 515–531, (2005).

[8] C. Mougenot et al., "Three-dimensional spatial and temporal temperature control with MR thermometry-guided focused ultrasound (MRgHIFU)," Magn. Reson. Med., vol. 61, no. 3, pp. 603–614, (2009).

[9] Z. Chen, "Bayesian filtering: From Kalman filters to particle filters, and beyond," Statistics (Ber)., vol. 182, no. 1, pp. 1–69, (2003).

[10] J. P. Kaipio and E. Somersalo, Statistical and Computational Inverse Problems. Springer Science+Business Media, Inc, (2004).

[11] H. R. B. Orlande et al., "State Estimation Problems in Heat Transfer," Int. J. Uncertain. Quantif., vol. 2, no. 3, pp. 239–258, (2012).

[12] D. Simon, Optimal State Estimation: Kalman, H Infinity, and Nonlinear Approaches. John Wiley & Sons, Inc., (2006).

[13] C. Pacheco, H. Orlande, M. Colaço, George S. Dulikravich, "State Estimation Problems in PRF-Shift Magnetic Resonance Thermometry", International Journal of Numerical Methods for Heat & Fluid Flow, (In press), (2018).

[14] Y. Ishihara et al., "A precise and fast temperature mapping using water proton chemical shift.," Magn. Reson. Med., vol. 34, no. 6, pp. 814–823, (1995).

[15] W. Wlodarczyk, R. Boroschewski, M. Hentschel, P. Wust, G. Mönich, and R. Felix, "Three-dimensional monitoring of small temperature changes for therapeutic hyperthermia using MR," J. Magn. Reson. Imaging, vol. 8, no. 1, pp. 165–174, (1998).

[16] R. W. Brown, Y. N. Cheng, E. M. Haacke, M. R. Thompson, and R. Venkatesan, Magnetic Resonance Imaging: Physical Principles and Sequence Design. Wiley, (1999).

[17] W. G. Schneider, H. J. Bernstein, and J. A. Pople, "Proton Magnetic Resonance Chemical Shift of Free (Gaseous) and Associated (Liquid) Hydride Molecules," J. Chem. Phys., vol. 28, no. 4, p. 601, (1958).

[18] J. C. Hindman, "Proton Resonance Shift of Water in the Gas and Liquid States," J. Chem. Phys., vol. 44, no. 12, p. 4582, (1966).

[19] R. Bitar et al., "MR Pulse Sequences: What Every Radiologist Wants to Know but Is Afraid to Ask," RadioGraphics, vol. 26, no. 2, pp. 513–537, (2006).

[20] V. Rieke, K. K. Vigen, G. Sommer, B. L. Daniel, J. M. Pauly, and K. Butts, "Referenceless PRF shift thermometry," Magn. Reson. Med., vol. 51, no. 6, pp. 1223–1231, (2004).

[21] H. H. Pennes, "Analysis of Tissue and Arterial Blood Temperatures in the Resting Human Forearm," J. Appl. Physiol., vol. 1, no. 2, pp. 93–122, Aug. (1948).

[22] L. A. B. Varon, H. R. B. Orlande, and G. E. Eliçabe, "Estimation of state variables in the hyperthermia therapy of cancer with heating imposed by radiofrequency electromagnetic waves," Int. J. Therm. Sci., vol. 98, pp. 228–236, (2015). [26] L. A. B. Varon, H. R. B. Orlande, and G. E. Eliçabe, "Combined parameter and state estimation in the radio frequency hyperthermia treatment of cancer," Numer. Heat Transf. Part A Appl., vol. 70, no. 6, pp. 581–594, (2016).

[23] M. S. Grewal and A. P. Andrews, Kalman Filtering: Theory and Practice Using MATLAB. Wiley, (2008).

[24] R. E. Kalman, "A new approach to linear filtering and prediction problems," Trans. ASME--Journal Basic Eng., vol. 82, no. Series D, pp. 35–45, (1960).

[25] P. Benner, V. Mehrmann, V. Sima, S. Van Huffel, and A. Varga, "SLICOT-A Subroutine Library in Systems and Control Theory," in Applied and Computational Control, Signals, and Circuits SE - 10, B. Datta, Ed. Birkhäuser Boston, pp. 499–539, (1999).

[26] M. J. Ackerman, "The Visible Human Project," Proc. IEEE, vol. 86, no. 3, pp. 504–511, (1998).

[27] P. A. Hasgall et al., "IT'IS Database for thermal and electromagnetic parameters of biological tissues," available: www.itis.ethz.ch/database. Website visited in 01/12/2017.